

Conditions for designing single-mode air-core waveguides in three-dimensional photonic crystals

Virginie Lousse^{a)}

Ginzton Laboratory, Stanford University, Stanford, California 94305 and Laboratoire de Physique du Solide, Facultés Universitaires Notre-Dame de la Paix, B-5000 Namur, Belgium

Jonghwa Shin and Shanhui Fan

Ginzton Laboratory, Stanford University, Stanford, California 94305

(Received 26 June 2006; accepted 30 August 2006; published online 17 October 2006)

The authors present a general procedure that allows the design of single-mode air-core waveguides in three-dimensional photonic crystals. The procedure involves analyzing the modal profile of the band edge mode in the perfect crystal, identifying the regions of maximal electric-field intensity, and placing the air defects to enclose these regions. As an illustration, they present a detailed design of air-core waveguides in a recently proposed silicon body-center-cubic crystal structure that possesses a 25% complete band gap. © 2006 American Institute of Physics. [DOI: 10.1063/1.2362983]

Recently, a lot of efforts have been concentrated on the holographic lithography fabrication technique¹⁻⁴ because of its ability to produce large-scale three-dimensional (3D) photonic crystals (PCs). 3D PCs with a complete band gap are attractive partly because they allow the creation of air-core waveguides on chip.⁵⁻¹² To use these air-core waveguides for integrated optics applications, one in addition needs these waveguides to be single moded and to possess a large bandwidth. Systematic investigations of air-core waveguiding structures in 3D holographic geometries have not been attempted yet.

While almost any air-core geometry can produce a guided mode in the gap, as we will show explicitly below, most of these geometries generate surfacelike modes, which have a very small bandwidth and most of the electric power in the high-dielectric regions at the surface of the waveguide. These modes are undesirable as they will strongly scatter in the presence of disorder. In this letter, we introduce a general procedure to avoid the formation of these surface modes. The procedure consists in examining the modal pattern of the band edge state in the perfect crystal, locating the regions of maximal electric-field intensity, and placing the air defects to enclose these regions. We will show that this procedure allows one to design single-mode air-core waveguides with a large bandwidth in 3D PCs.

To illustrate this procedure, we consider a body-centered-cubic (bcc) gyroid structure similar to that in Refs. 3, 4, and 13, compatible with the holographic fabrication technique. The silicon structure is defined by

$$\varepsilon(x, y, z) = 12.06 \quad \text{if } \sin(2\pi(x+y)/a) + \sin(2\pi(x-y)/a) \\ + \sin(2\pi(y+z)/a) + \sin(2\pi(y-z)/a) \\ + \sin(2\pi(z+x)/a) + \sin(2\pi(z-x)/a) > 2.0,$$

$$\varepsilon(x, y, z) = 1 \quad \text{otherwise,}$$

where a is the length of the cubic unit cell. Figure 1 shows the dielectric constant distribution in a single cubic unit cell. This structure, with a filling ratio of 17%, gives rise to a 25%

band gap between the second and third bands in the band diagram.¹³

Almost any line defect structure in a 3D complete band gap PC behaves as a waveguide. However, most of these waveguides are in fact not optimal for integrated optics applications. In this work, we consider line defects oriented along the z axis ([001] direction). We carry out a full analysis of the defect modes with the plane-wave expansion method, where Maxwell's equations are solved in the frequency domain.¹⁴ To calculate the dispersion relations of the waveguides modes, we use a supercell with the size $5a \times 5a \times a$ and approximately 820 000 plane waves. This supercell size guarantees a convergence of frequency to an accuracy of 0.01%, as tested by comparing to a $7a \times 7a \times a$ supercell at a single \mathbf{k} point. The first waveguiding structure we consider is an air cylinder of radius $R=0.25a$ centered at $(0, 0, 0)$ in the cubic unit cell of the bcc structure. This structure gives rise to flat bands in the photonic band gap [see Fig. 2(a)], with the maxima of electric-field energy located in the high dielectric regions at the surface of the waveguide [see inset of Fig. 2(a)].

The origin of these surfacelike modes can be understood by analyzing the behavior of the bulk modes of a perfect crystal. As introducing an air defect in a PC has the effect to push the bands right below the gap into the band gap,¹⁵ we examine the distribution of the fields for the two degenerate

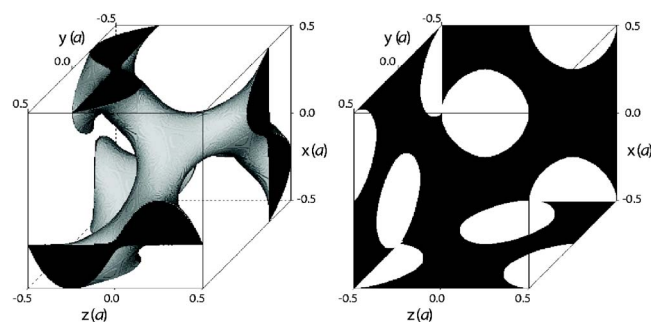


FIG. 1. (Color online) Dielectric constant of the bcc structure, plotted in the cubic unit cell of length a . The gray regions represent Si. Plotted in black on the right panel are the maxima of dielectric constant projected on the three Cartesian planes.

^{a)}Electronic mail: virginie.lousse@stanford.edu

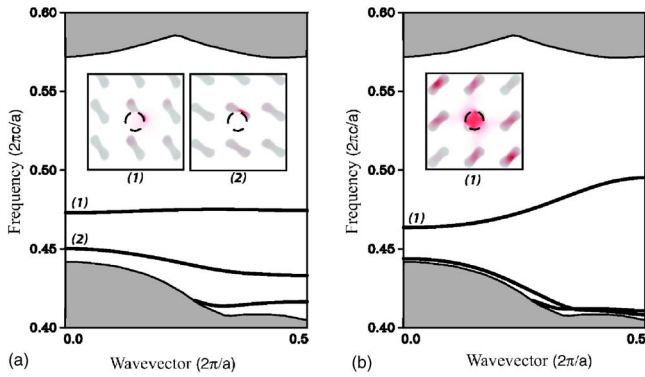


FIG. 2. (Color online) Band structures for waveguides in the bcc gyroid crystal. The shaded areas indicate the propagating modes in the perfect three-dimensional photonic crystal. The linear defects are along the z direction. (a) The linear defect is an air cylinder of radius $R=0.25a$ centered at $(0,0,0)$. (b) The linear defect is made of an array of air spheres of radius $R=0.25a$. The spheres are centered in the high-intensity regions at $c_a = (0, a/4, a/8)$. The insets of these two figures show the energy in the electric field at the Brillouin zone center for the modes in the band gap. At the center of each plot, the circle represents the position of the air defect introduced.

bulk modes right below the band gap in the projected band diagram. Figure 3 shows the maximum energy in the electric field at the Brillouin zone center for these two modes. The maxima of energy are projected on the three Cartesian planes and are concentrated in the high-dielectric material in special points labeled $a-f$ in Fig. 3. These high-intensity regions can be approximated as spheres, with centers respectively located at

$$\begin{aligned}
 c_a &= (0, a/4, a/8), \\
 c_b &= (0, -a/4, 3a/8), \\
 c_c &= (3a/8, 0, -a/4), \\
 c_d &= (a/4, a/8, 0), \\
 c_e &= (a/8, 0, a/4), \\
 c_f &= (a/4, -a/8, a/2).
 \end{aligned}
 \tag{1}$$

In 3D PCs, the surfacelike modes arise when the air defect edge cuts through dielectric material where the band edge modes have a high electric-field intensity. When the pertur-

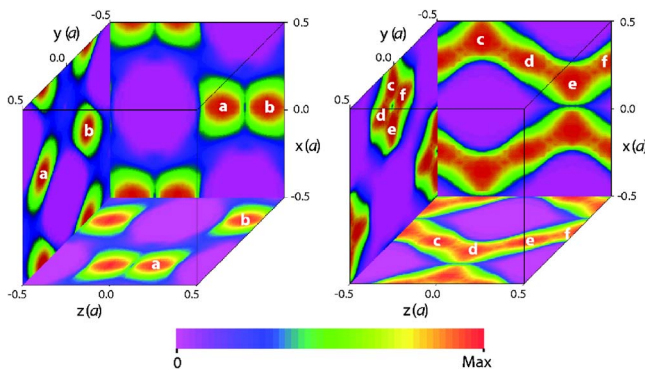


FIG. 3. (Color online) Energy in the electric field for the bulk modes in the two bands right below the gap at the Brillouin zone center. Plotted here are the maxima of energy projected on the three Cartesian planes. The areas labeled $a-f$ correspond to the high-energy regions.

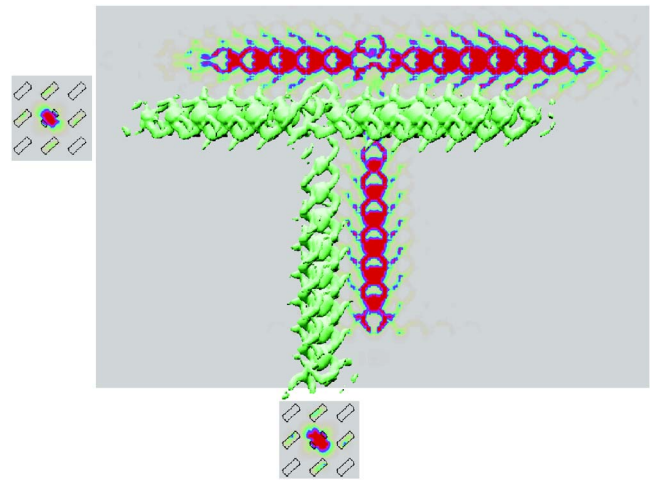


FIG. 4. (Color online) Large angle splitter, demonstrated by a FDTD simulation. The structure has a vertical waveguide made by removing dielectric regions corresponding to label a in Fig. 3, and a horizontal waveguide made by removing dielectric regions corresponding to label d .

bation is an air cylinder of radius $R=0.25a$ centered at $(0, 0, 0)$ in the cubic unit cell of the bcc structure, the waveguiding structure is cutting through the high-intensity regions labeled a and b in Fig. 3, which gives rise to flat bands in the projected band diagram [Fig. 2(a)]. Similar mechanisms have been previously observed in photonic-band-gap fibers,¹⁶ 2D PCs,^{15,17} or self-assembled PCs.¹²

Based on this analysis, we propose a way to design single-mode air-core waveguides. To avoid cutting through the high-intensity regions, the waveguiding structures in the rest of this work are created by placing air spheres centered at the maxima of the high-intensity spots in the crystal. The radii of these air spheres are chosen so that each of them completely encloses one high-intensity region. Figure 2(b) shows the projected band structure for a line defect made of an array of air spheres of radius $R=0.25a$ centered on $c_a + n\mathbf{z}$, where $n=0, 1, 2, \dots$ and \mathbf{z} is a unit vector in the z direction. Each primitive unit cell of the waveguide contains one sphere. We observe that removing one complete high-intensity region in the cubic unit cell gives rise to a single defect mode in the photonic band gap. This defect band extends across the entire Brillouin zone, inside the band gap, and exhibits vanishing group velocity at both the center and the edge of the Brillouin zone. The waveguiding bandwidth reaches 102 nm centered at a wavelength of $1.5 \mu\text{m}$ and the waveguide mode exhibits a band center group velocity of approximately $0.12c_0$, where c_0 is the velocity of light in vacuum. The inset of Fig. 2(b) shows that this mode possesses a large fraction of energy in air. In particular, the maximum of the electric-field intensity is in air at the center of the waveguide.

The propagation of the electromagnetic waves through a large-angle splitter using this optimal single-mode air waveguide is analyzed with the finite-difference time-domain method¹⁸ (FDTD) (see Fig. 4). Simulations are done with ten grid points per period and the guided mode is excited with an array of point sources inside the waveguide. The structure has a vertical (z directional) waveguide made by removing dielectric regions corresponding to the label a in Fig. 3, and a horizontal (y directional) waveguide made by removing dielectric regions corresponding to label d . The d region is equivalent to the a region with the change of the propagation

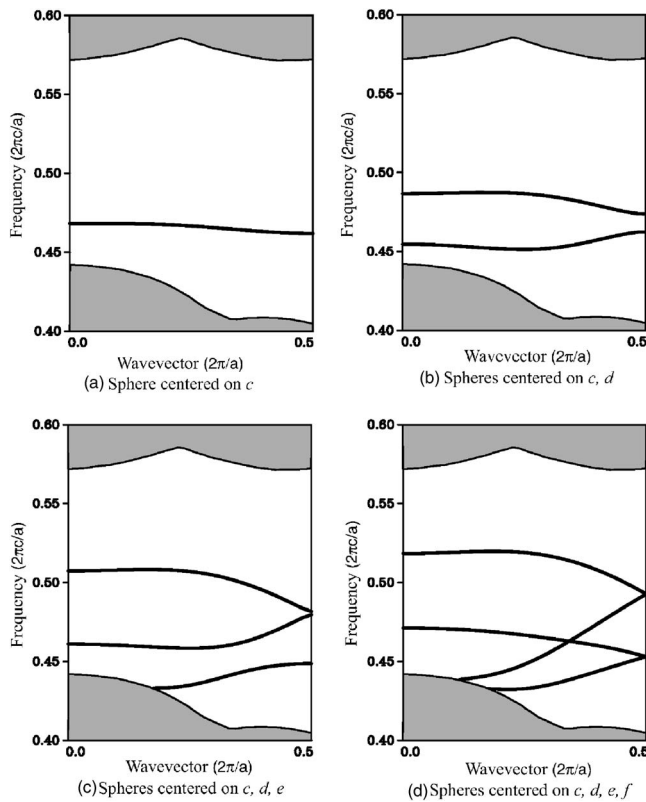


FIG. 5. Band structures for waveguides in the bcc gyroid crystal. The shaded areas indicate the propagating modes in the perfect three-dimensional photonic crystal. The linear defects are made of arrays of air spheres along the z direction. The spheres of radius $R=0.2a$ are centered in the high-intensity regions labeled in Fig. 3.

direction. A guided mode is launched from the bottom port by a narrow bandwidth temporal Gaussian pulse with a center frequency $0.48 (2\pi c/a)$, and snapshots of the electric field energy are taken after sufficient time steps. The entire crystal is $6a \times 20a \times 13a$ in size and is placed within a thin layer of air with absorbing boundary conditions outside. (Due to the reflections from the air-crystal interface, the plot is not representative of actual splitting ratio.) As expected, a significant fraction of energy is found in the air region labeled a and d , respectively, for the two waveguides, with no radiation loss out of the waveguiding structure.

This understanding also enables us to control the number of bands pushed into the gap. As an illustration, we consider waveguides made by removing spheres of dielectric covering the high-energy regions of the band edge mode, labeled $c-f$ in Fig. 3. The projected band diagrams in Figs. 5(a)–5(d) are obtained for defects created by removing one to four high-intensity spots per cubic unit cell, respectively. In general, the number of defect modes present in the band gap is equal to the number of high-energy regions removed per unit cell. By varying the radius of the spherical air defects, we have

also observed that the bandwidth of these defect modes increases with the portion of dielectric removed in the structure.

In conclusion, this study suggests a general procedure to avoid the formation of surfacelike modes and to predict the number of defect modes in the photonic band gap. It simply consists in a computation of the intensity profile of the bulk mode right below the gap and an evaluation of the spatial overlap between this profile and the air defect, instead of a full calculation of the defect modes. As an illustration, we presented here the design of air-core waveguides in a bcc crystal, compatible with the holographic lithography technique. This procedure, however, is general and it has proven to be valid for a whole range of 3D PC structures. In particular, we have found that it could be used to design single-mode air-core waveguides in lithographically defined layer-by-layer crystals, or to avoid surfacelike modes in self-assembled opal structures.

The work was supported in part by the Department of Defense Multidisciplinary University Research Initiative (ARO-MURI) Grant No. DAAD19-03-1-0227. The simulations were performed through the support of the National Science Foundation (LRAC program). One of the authors (J.S.) acknowledges a Samsung Lee Kun Hee Scholarship and another author (V.L.) was supported as Postdoctoral Fellow by the Belgian National Fund for Scientific Research (FNRS).

¹M. Campbell, D. N. Sharp, M. T. Harrison, R. G. Denning, and A. J. Turberfield, *Nature (London)* **404**, 53 (2000).

²L. Z. Cai, X. L. Yang, and Y. R. Wang, *Opt. Lett.* **27**, 900 (2002).

³O. Toader, T. Y. M. Chan, and S. John, *Phys. Rev. Lett.* **92**, 043905 (2004).

⁴C. K. Ullal, M. Maldovan, E. L. Thomas, G. Chen, Y. Han, and S. Yang, *Appl. Phys. Lett.* **84**, 5434 (2004).

⁵A. Chutinan and S. Noda, *Appl. Phys. Lett.* **75**, 3739 (1999).

⁶S. Noda, K. Tomoda, N. Yamamoto, and A. Chutinan, *Science* **289**, 604 (2000).

⁷M. L. Povinelli, S. G. Johnson, S. Fan, and J. D. Joannopoulos, *Phys. Rev. B* **64**, 075313 (2001).

⁸Z. Y. Li and K. M. Ho, *J. Opt. Soc. Am. B* **20**, 801 (2003).

⁹C. Sell, C. Christensen, J. Muehlmeier, G. Tuttle, Z. Y. Li, and K. M. Ho, *Appl. Phys. Lett.* **84**, 4605 (2004).

¹⁰A. Chutinan and S. John, *Phys. Rev. E* **71**, 026605 (2005).

¹¹A. Chutinan and S. John, *Opt. Express* **14**, 1266 (2006).

¹²V. Lousse and S. Fan, *Opt. Express* **14**, 866 (2006).

¹³J. Shin and S. Fan, *Opt. Lett.* **30**, 2397 (2005).

¹⁴S. G. Johnson and J. D. Joannopoulos, *Opt. Express* **8**, 173 (2001).

¹⁵J. D. Joannopoulos, R. D. Meade, and J. N. Winn, *Photonic Crystals, Molding the Flow of Light* (Princeton University Press, Princeton, NJ, 1995).

¹⁶H. K. Kim, J. Shin, S. Fan, M. J. F. Digonnet, and G. S. Kino, *IEEE J. Quantum Electron.* **40**, 551 (2004).

¹⁷W. T. Lau and S. Fan, *Appl. Phys. Lett.* **81**, 3915 (2002).

¹⁸K. S. Kunz and R. J. Luebbers, *The Finite-Difference Time-Domain Methods for Electromagnetics* (CRC, Boca Raton, FL, 1993).